



**HAL**  
open science

## Detailed structural elucidation of different lignocellulosic biomass types using optimized temperature and time profiles in fractionated Py-GC/MS

María González Martínez, T. Ohra-Aho, T. Tamminen, D. da Silva Perez, M. Campargue, C. Dupont

### ► To cite this version:

María González Martínez, T. Ohra-Aho, T. Tamminen, D. da Silva Perez, M. Campargue, et al.. Detailed structural elucidation of different lignocellulosic biomass types using optimized temperature and time profiles in fractionated Py-GC/MS. *Journal of Analytical and Applied Pyrolysis*, 2019, 140, pp.112 - 124. 10.1016/j.jaap.2019.02.011 . hal-03484969

**HAL Id: hal-03484969**

**<https://hal.science/hal-03484969>**

Submitted on 20 Dec 2021

**HAL** is a multi-disciplinary open access archive for the deposit and dissemination of scientific research documents, whether they are published or not. The documents may come from teaching and research institutions in France or abroad, or from public or private research centers.

L'archive ouverte pluridisciplinaire **HAL**, est destinée au dépôt et à la diffusion de documents scientifiques de niveau recherche, publiés ou non, émanant des établissements d'enseignement et de recherche français ou étrangers, des laboratoires publics ou privés.



Distributed under a Creative Commons Attribution - NonCommercial 4.0 International License

## Detailed structural elucidation of different lignocellulosic biomass types using optimized temperature and time profiles in fractionated Py-GC/MS

M. González Martínez<sup>a,b,c,\*</sup>, T. Ohra-aho<sup>d</sup>, T. Tamminen<sup>d</sup>, D. da Silva Perez<sup>e</sup>, M. Campargue<sup>f</sup>, C. Dupont<sup>g</sup>

<sup>a</sup> Université Grenoble Alpes, CEA, Laboratoire de Préparation des Bioressources (LPB), F-38000 Grenoble, France

<sup>b</sup> Université de Toulouse; INPT, UPS; Laboratoire de Génie Chimique, 4 Allée Emile Monso, F-31030 Toulouse, France

<sup>c</sup> CNRS; Laboratoire de Génie Chimique; F-31030 Toulouse, France

<sup>d</sup> VTT Technical Research Centre of Finland Ltd, P.O. Box 1000, FI-02044 VTT, Finland

<sup>e</sup> FCBA, InTechFibres Division, CS 90251, F-38044, Grenoble, France

<sup>f</sup> RAGT Energie, zone Innoprod, Chemin de la Teulière, F-81000 Albi, France

<sup>g</sup> IHE Delft Institute for Water Education, Department of Environmental Engineering and Water Technology, Delft, The Netherlands

\*Corresponding author: [maria.gonzalez-martinez@outlook.com](mailto:maria.gonzalez-martinez@outlook.com) (M. González Martínez)

### Abstract

Fractionated pyrolysis coupled to gas chromatography and mass spectrometry experiments (Py-GC/MS) were carried out on eight woody and agricultural biomasses, including beech, poplar, pine forest residues, Scot Pine bark, reed canary grass, corn cob, grape seed cake and wheat straw. The selected temperature and duration for each fractionated pyrolysis step allowed separating the volatile pyrolysis products in function of their origin from biomass. As a result, carbohydrate derivatives from hemicelluloses were released at earlier fractionated pyrolysis steps, compared to those produced from cellulose degradation. Phenolic derivatives, mainly produced by lignin, were stepwise produced in function of the length and the nature of their side-chain substituents. Protein derivatives were also released in the whole Py-GC/MS temperature range. Macromolecular composition and biomass family were shown to play a crucial role in the thermal degradation of the biomasses of study. Production profiles exhibited resemblances per chemical species between deciduous and coniferous woods, while they appear to be more heterogeneous for agricultural biomasses. Herbaceous crops showed an intermediate behaviour between woods and agricultural biomasses.

### Highlights

- Thermal degradation of eight biomasses was evaluated by fractionated Py-GC/MS.
- Volatile production profiles contribute in biomass structure elucidation.
- Macromolecular composition strongly affects thermal degradation.
- The maximum of carbohydrate derivatives profiles suggests their origin.
- Release order of lignin phenolics were from long to short side-chain.

## 35 **Keywords**

- 36 • Py-GC/MS
- 37 • Fractionated pyrolysis
- 38 • Lignocellulosic biomass
- 39 • Lignin
- 40 • Carbohydrates

## 41 **1. INTRODUCTION**

42 Lignocellulosic biomass, including woody, agricultural and herbaceous resources, has been shown to play a  
43 strategic role in the current transformation of the energetic production [1]. Its macromolecular composition  
44 consists mainly of cellulose, hemicelluloses and lignin, with water, minor amounts of proteins, pectins, minerals  
45 and other trace components [2]. While cellulose and hemicelluloses are based on various monosaccharides,  
46 lignin is an oxygenated polymer based on phenylpropane units [3]. The proportions and distribution of these  
47 macromolecular components in biomass physical structure is complex and dependent on biomass type.  
48 Interactions between cellulose, hemicelluloses and lignin in biomass have been demonstrated to play a role in  
49 its thermochemical conversion [4–6].

50 Cellulose is a major structural component of cell walls, which provides mechanical strength and chemical  
51 stability to lignocellulosic biomass. It is present in biomass as microfibrils consisting of a semi-crystalline  
52 macromolecular structure formed by a long straight chain of (1,4)-D-glucopyranose units linked by  $\beta$ -1,4  
53 glycosidic bond [2,7,8]. Glucan chains composing cellulose are linked together through extensive hydrogen  
54 bonding, forming linear organized arrays of chains. The order in the glucan chains in the microfibrils is  
55 sometimes altered, leading to disordered areas along the length of microfibrils. These more likely-amorphous  
56 regions are suspected to be more propitious to the association of hemicelluloses with cellulose microfibrils [9].

57 Hemicelluloses are heteropolysaccharides formed by several types of sugar molecules composed either of  
58 five or six carbon atoms. In the first case, pentose sugars are the basis of the structure (arabinose, xylose),  
59 while in the second case hexose sugars constitute hemicelluloses (galactose, glucose and mannose).  
60 Hexuronic acids (e.g. glucuronic acid) can also be present in the structure, as well as acetyl groups connected  
61 to the chain, usually to xylans and arabinoxylans [9]. The function of hemicelluloses is to contribute to the  
62 formation of a resistant and cohesive network of cellulose microfibrils. The structure of hemicelluloses is  
63 conditioned by the main sugar involved in the polymer construction, the frequency and the nature of the  
64 ramifications and the degree of polymerization [10].

65 Lignin structural units are represented by *p*-hydroxyphenyl (H), guaiacyl (G) and syringyl (S) units. These units  
66 are derived from the copolymerization of *p*-coumaryl alcohol, coniferyl alcohol and sinapyl alcohol, respectively  
67 [11]. Important differences exist between lignin structure from hardwood (angiosperm) and softwood  
68 (gymnosperm). Lignin from softwood is mostly formed by G-units and some H-units, mainly, while lignin  
69 constituting hardwood contains varying ratios of G-and S-units [12]. Lignin in poplar differs from the other  
70 hardwoods as it contains *p*-hydroxybenzoic acid linked to lignin [13]. On the contrary, lignin from herbaceous  
71 plants contains three types of units (H, S and G) [14]. The lignin structure of agricultural biomasses is more  
72 complex and contains G-and H-units. In addition, these biomasses often contain *p*-hydroxycinnamic acids (*p*-

73 coumaric and ferulic acids) [15]. The role of *p*-hydroxycinnamic acids in herbaceous biomasses was described  
74 as a bridge between lignin and carbohydrates through LCC (lignin-carbohydrates complexes) [16]. As a result,  
75 these acids were not considered as part of the lignin structure. In addition, some proteins can be present in  
76 agricultural biomasses [17,18]. Lignin function is forming a protective layer for the plant walls by encasing  
77 cellulose and hemicellulose of the cell walls [2]. At the same time, covalent bonds between hemicellulose and  
78 lignin provide resistance to the structured microfibrillar network of the plant [19,20].

79 Structurally, significant differences exist between hardwood and softwood in cell structure, concerning  
80 complexity and cell types. More precisely, softwoods present a simpler structure with only two cell types which  
81 are mainly invariable. Hardwoods are characterized by a higher degree of variability within a higher number of  
82 cell types, presenting also a characteristic type of cell (vessel element or pore), which is absent in softwoods  
83 [21,22]. In both cases, tissues of woody biomasses contain the main part of lignin in the secondary cell wall  
84 layers [23]. Even if the cell structure of agricultural biomasses and herbaceous crops is close to that of  
85 hardwood, the main differences concern the macromolecular components forming the cell walls, how they are  
86 linked together, and the abundance and nature of pectins, proteins and phenolic compounds [24].

87 Analytical pyrolysis coupled to gas chromatography and mass spectrometry (Py-GC/MS) has largely been  
88 used during the last decades in the elucidation of biomass structure [14,25–28]. This consists of biomass flash  
89 heating at rates higher than  $10,000 \text{ K}\cdot\text{s}^{-1}$  up to pyrolysis temperatures, typically between 400 to 600 °C. The  
90 pyrolysis degradation products, released as volatile species, are then separated, identified and quantified in  
91 GC/MS. The production profiles of the released degradation products contribute to explain their origin from  
92 macromolecular components in biomass structure. Previous studies including Py-GC/MS simultaneously  
93 analyzed a reduced number of biomasses, which were typically from the same biomass family [15,27,29–33].  
94 The use of an optimized temperature and time configuration in fractionated Py-GC/MS experiments was shown  
95 to separate pyrolysis products according to their origin from lignin and carbohydrate degradation. At the same  
96 time, the yield of pyrolysis products released was shown to be maximized under these conditions and the  
97 extent of the secondary in gaseous phase is expected to be minimized [34].

98 The objective of this work is the broadening of the use of fractionated Py-GC/MS with an optimized temperature  
99 and time configuration to the elucidation of the structure of woody and agricultural biomasses, linked to their  
100 macromolecular composition. All together eight biomasses were studied. The distribution of the volatile  
101 pyrolysis products grouped per chemical family and through the seven steps of the fractionated pyrolysis  
102 experiments was firstly studied. In a second step, the formation of volatile pyrolysis products was analysed in  
103 function of their repartition in each step of the fractionated Py-GC/MS and in function of the biomass type.  
104 Pyrolysis products derived from carbohydrates, lignin and proteins were monitored. Special attention was paid  
105 to the correct identification of the source of some degradation products that may be derived from several  
106 components, such as *p*-hydroxyphenyl derivatives (protein/lignin/*p*-hydroxybenzoic acid) and vinyl derivatives  
107 (cinnamic acids/lignin). As the aim of the study was to simulate the reactions occurring in thermal processing,  
108 samples were analyzed as they were available, without washing, and the role of inorganic components, which  
109 was the object of previous studies in the literature [35,36], was not assessed in this case.

## 110 2. MATERIAL AND METHODS

112 Eight biomasses, representative of the European diversity, were selected for fractionated Py-GC/MS  
 113 experiments. This includes two deciduous woods (beech, poplar), a coniferous wood (pine forest residues), a  
 114 coniferous wood bark (Scot pine bark), three agricultural by-products (corn cob, grape seed cake and wheat  
 115 straw) and one herbaceous crop (reed canary grass).

116 Poplar and beech were harvested by thinning cut in the South of France in the summer 2016. Pine forest  
 117 residues and Scot pine bark were prepared in Sweden in the summer 2015. Wheat straw was harvested in the  
 118 South of Sweden in autumn 2015. Finally, corn cob and grape seed cake corresponded to residues collected  
 119 in October 2015 from seed and oil plants (RAGT, France), which use raw biomasses from the South of France.

120 Woody biomasses were first convectively dried by blowing heated air (40–60 °C) through a perforated floor,  
 121 until all the material reached about 5% moisture content (water basis, w.b.). Agricultural biomasses were not  
 122 dried. All woody and agricultural biomasses, except grape seed cake, were then shredded with a Lindner  
 123 Micromat 2000 (Linder-Recyclingtech GmbH, Spittal, Austria) with 15 mm screen size. Finally, all biomasses  
 124 were ground at a particle size inferior to 500 µm using a Universal cutting mill Fritsch Pulverisette 19 (Fritsch  
 125 GmbH, Idar-Oberstein, Germany) with a 0.5mm sieve. No pretreatment was applied to remove extractives and  
 126 inorganic elements (ash) prior to pyrolysis experiments.

127 Biomasses were characterized in terms of macromolecular composition (Table 1) and sugar distribution (Table  
 128 2) according to methods described previously in [37]. Comments on this characterization are already reported  
 129 in [38]. Nitrogen content was measured through the Standard XPCEN/TS 15107. Protein content was  
 130 determined by multiplying nitrogen content by a factor 6.25, as protein is mainly precipitated in acid hydrolysis  
 131 together with lignin [17]. Therefore, lignin content was corrected by subtracting with protein content.

132 **Table 1. Macromolecular composition of the biomasses**

<b>Biomass</b>	<b>Cellulose</b>	<b>Hemicell</b>	<b>Lignin</b>	<b>Protein</b>	<b>Extractives</b>	<b>Inorganics (ash)</b>	<b>Mass balance</b>
	<b>% wmf*</b>						
<b>Deciduous wood</b>							
Beech	41.3	25.3	25.2	1.3	1.9	0.8	95.7
Poplar	42.7	21.8	25.6	1.3	4.4	2.8	98.5
<b>Coniferous wood</b>							
Pine forest residues	22.3	27.9	23.1	4.4	18.9	2.2	98.8
Scot pine bark	21.9	18.3	38.2	2.5	15.2	2.8	98.9
<b>Herbaceous crops</b>							
Reed canary grass	39.5	25.7	20.3	4.4	6.4	6.6	102.8
<b>Agricultural by-products</b>							
Corn cob	38.4	34.8	13.4	2.5	6.9	1.9	97.7
Grape seed cake	7.8	21.9	47.2	15.6	7.6	4.2	104.2
Wheat straw	38.1	24.7	19.3	3.1	7.8	9.3	102.3

\*% wmf = weight-moisture-free

133 **Table 2. Neutral monosugars distribution and functional groups**

	Neutral sugars balance (normalized)					Functional groups
	Glucose	Xylose	Mannose	Galactose	Arabinose	Acetyl groups
<b>Biomass</b>			%*			% wmf**
<b>Deciduous wood</b>						
Beech	63.9	29.1	3.0	2.0	2.0	8.3
Poplar	68.9	22.7	4.3	2.0	2.2	5.9
<b>Coniferous wood</b>						
Pine forest residues	58.8	10.7	14.4	8.7	7.5	2.7
Scot pine bark	64.3	7.9	9.9	7.1	10.9	1.6
<b>Herbaceous crops</b>						
Reed canary grass	61.0	29.9	0.4	3.1	5.6	5.0
<b>Agricultural by-products</b>						
Corn cob	52.4	39.4	0.0	2.5	5.7	5.0
Grape seed cake	33.6	48.2	7.4	5.2	5.6	3.1
Wheat straw	61.0	32.5	0.3	1.6	4.6	3.7

\*% of the total monosugars; \*\*% wmf = weight moisture free

134

135

## 2.2. PY-GC/MS EXPERIMENTS

136

137

138

139

140

141

142

Py-GC/MS measurements were performed with a filament pulse pyrolyzer (Pyrola2000. PyrolAB. Sweden) connected to a gas chromatograph (Agilent 7890B) with a mass spectrometer (Agilent 5977A). A detailed description of the fractionated pyrolysis conditions has been included in a previous work [34]. To sum up, about 100 µg of the biomass sample was weighed accurately and placed on the platinum filament in the pyrolyzer sample holder. Each sample was pyrolyzed according to the fractionated pyrolysis program of temperatures and times indicated in Table 3. The most suitable time at each temperature was set in preliminary experiments with beech, by checking that all volatile species are released at each pyrolysis step [34].

143

144

**Table 3. Time set at each step of fractionated pyrolysis experiments (Py-GC/MS) for the selected temperatures**

step	temperature (°C)	time (s)
1	250	40
2	300	30
3	350	25
4	370	20
5	400	15

6	450	10
7	500	5

145

146 At each pyrolysis temperature, 0.008 s was the time set to reach a given pyrolysis temperature ( $\approx 50,000$  K·s<sup>-1</sup>).  
 147 After each step of the fractionated pyrolysis degradation products were swept with helium into the gas  
 148 chromatography for separation using a mid-polar capillary column (J&W. DB-1701. 30 m  $\times$  0.25 mm. film 1  
 149  $\mu$ m). After separation, degradation products were detected using a quadrupole mass spectrometry (EI 70 eV).  
 150 Each experiment was carried out twice, which confirmed the repeatability of the results.

151 Table 4 includes volatile species released in fractionated pyrolysis of the eight selected biomasses and  
 152 detected in GC/MS analysis. Pyrolysis products could be identified thanks to data from the literature [39–42],  
 153 as well as to the commercial NIST 2011 MS library, by considering a correct identification for a Match/RMatch  
 154 higher than 900.

155 **Table 4. Chemical compounds followed using extracted ion (EI) in GC/MS analysis of the volatile**  
 156 **species released in the fractionated pyrolysis of different biomasses**

Chemical compound	EI	Chemical compound	EI
<b>Guaiacyls</b>		<b>Anhydrosugars (and dihydropyranoses)</b>	
3-methylguaiacol	123	1,4-anhydroxylopyranose	57
guaiacol	124	1,5-anhydroarabinofuranose	57
homovanillin	137	1,6-anhydroglucopyranose (levoglucosan)	60
4-ethylguaiacol	137	1,4-anhydrogalactopyranose	73
4-(1-hydroxy-prop-2-enyl)guaiacol	137	1,5-anhydro-4-deoxypent-1-en-3-ulose	114
4-methylguaiacol	138	1,4-dideoxy-D-glycero-hex-1-enopyranos-3-ulose	144
vanillin	151	<b>Acids</b>	
acetoguaiacone	151	acetic acid	60
eugenol	164	<b>Furans</b>	
<i>cis</i> -isoeugenol	164	2(5H)-furanone	55
<i>trans</i> -isoeugenol	164	5-hydroxymethyldihydrofuran-2-one	85
dihydroconiferyl alcohol	137	furfural	96
<i>trans</i> -coniferyl alcohol	180	5-hydroxymethylfurfural	97
<b>Syringyls</b>		2-furanmethanol	98
syringol	154	<b>Ketones</b>	
syringylacetone	167	hydroxyacetone	43
4-ethylsyringol	167	1,2-cyclopentanedione	98
homosyringaldehyde	167	2-hydroxy-3-methyl-2-cyclopenten-1-one	112
4-methylsyringol	168		
acetosyringone	181	<b>Protein derivatives</b>	
syrialdehyde	182	indole	117
4-allylsyringol	194	methylindole	130
4-propenylsyringol	194		
<b><i>p</i>-hydroxyphenyls</b>		<b>Vinyl derivatives</b>	
phenol	94	4-vinylphenol	120

4-methylphenol	107	4-vinylguaiacol	150
2-methylphenol	108	4-vinylsyringol	180

157

158 Peak areas of pyrolysis products were integrated using extracted-ion chromatogram (EIC) with the selected  
 159 ion for each compound (Table 4). Then, peak areas were normalized considering the weight of the sample.  
 160 The average of two parallel measurements was calculated for each point. The estimated standard error for  
 161 parallel measurements was below 10%. Peak area in the chromatogram was the selected magnitude for the  
 162 data analysis, due to the impossibility of calibrating all detected chemical species.

163 In a first step, pyrolysis products were grouped per chemical family and their peak areas were added. The  
 164 production ratio per chemical family at each fractionated pyrolysis step was calculated as a ratio of the total  
 165 production of volatile species of the given step (Figure 1). The addition of peak areas of different volatile species  
 166 belonging to the same chemical family can only be considered for comparing trends between families and/or  
 167 biomasses.

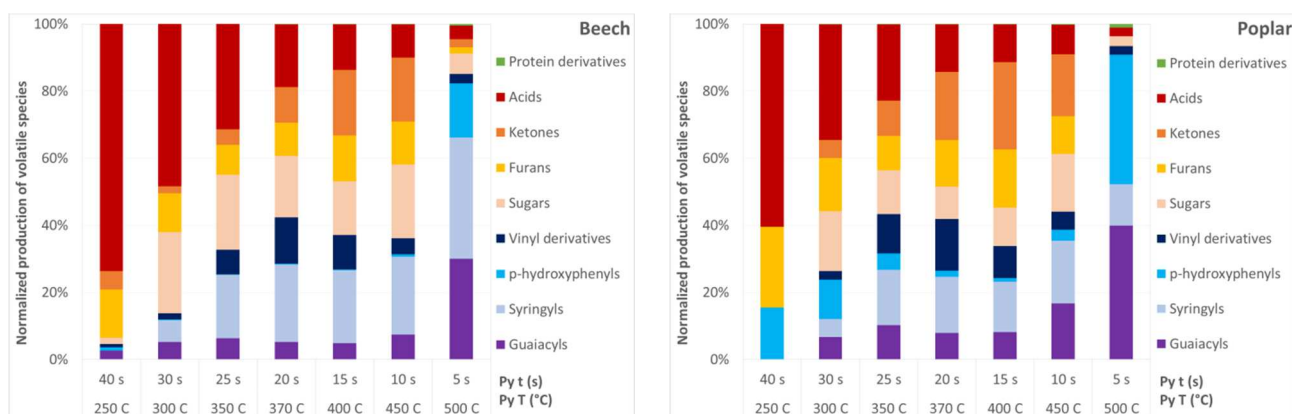
168 Secondly, the production profile of each pyrolysis product was shown versus temperature and step duration.  
 169 The production of the pyrolysis product was calculated for each step of the fractionated pyrolysis as the  
 170 percentage of the total production of the given species in the seven steps of fractionated pyrolysis (Figures 2  
 171 to 10).

### 172 3. RESULTS AND DISCUSSION

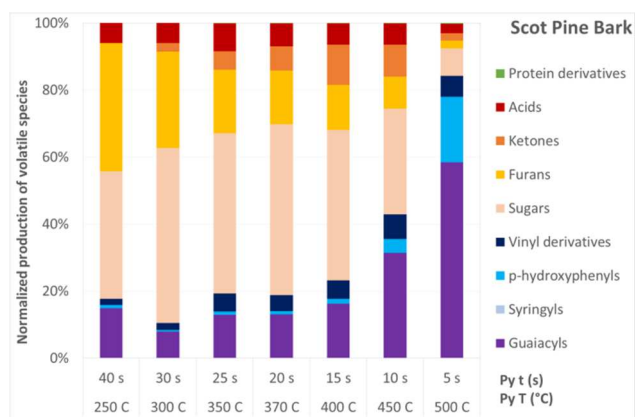
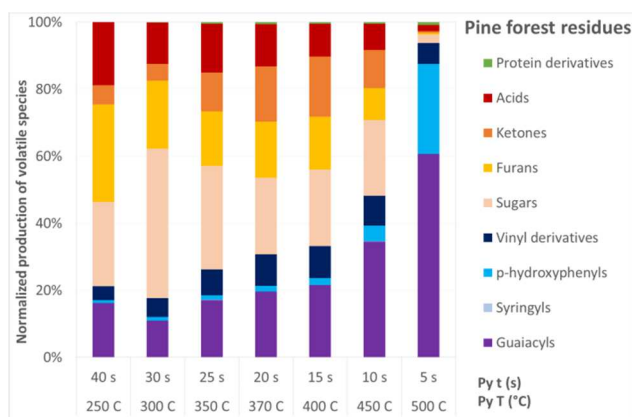
#### 173 3.1. ANALYSIS OF THE VOLATILE SPECIES RELEASED PER BIOMASS

174 The production of volatile species per chemical family released in the Py-GC/MS experiments with different  
 175 biomasses was compared (Figure 1). Biomasses were grouped by families: deciduous wood (beech, poplar),  
 176 coniferous wood and its bark (pine forest residues, Scot pine bark) and agricultural by-products, including  
 177 herbaceous crops (corn cob, grape seed, cake, reed canary grass, wheat straw).

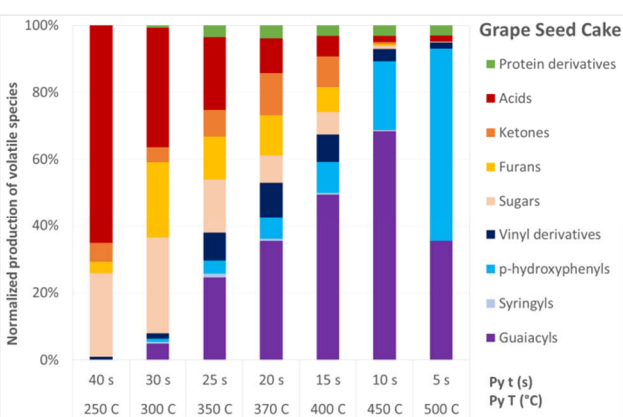
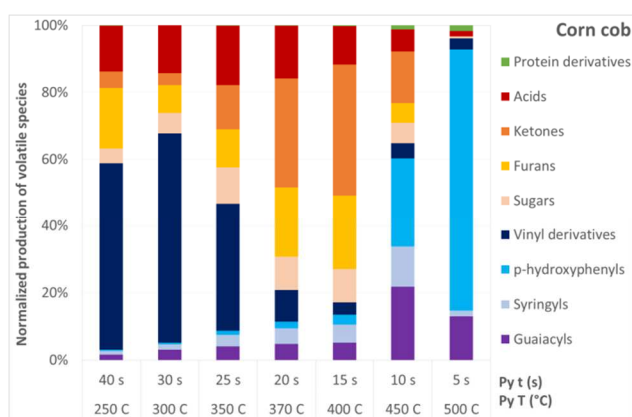
178



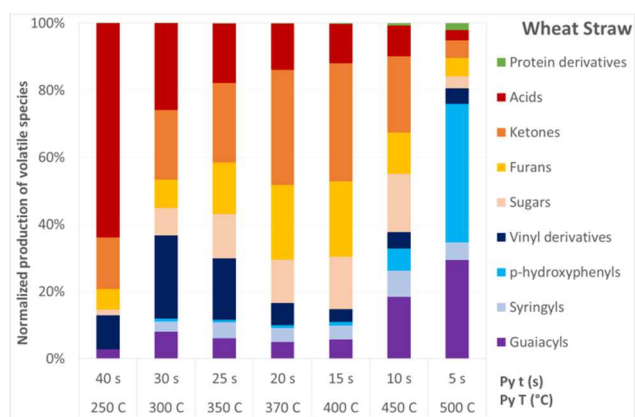
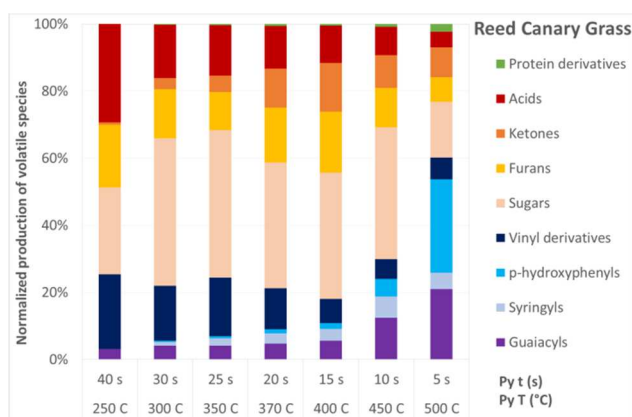
179



180



181



182 **Figure 1. Total production of volatile species classified in chemical families and normalized per**  
 183 **temperature in the fractionated fast pyrolysis of the eight selected biomasses in Py-GC/MS**

184 The pyrolysis product distribution varied with biomass type and fractionated pyrolysis step. Similar distribution  
 185 could be observed per duration/temperature step for biomasses from the same family, particularly for  
 186 deciduous and coniferous wood. This distribution is more heterogeneous for agricultural biomasses, including  
 187 herbaceous crops, presumably because of their more heterogeneous macromolecular composition compared  
 188 to woods (Table 1).

189 However, wheat straw, corn cob and reed canary grass showed similarities in product distribution, which is  
 190 probably due to their rather similar macromolecular structure. These biomasses differed from the woody  
 191 biomasses and grape seed cake releasing a high proportion of vinyl derivatives in the low temperature region  
 192 (250-350 °C). The result indicated the presence of hydroxycinnamates, in which *p*-coumaric acid has been

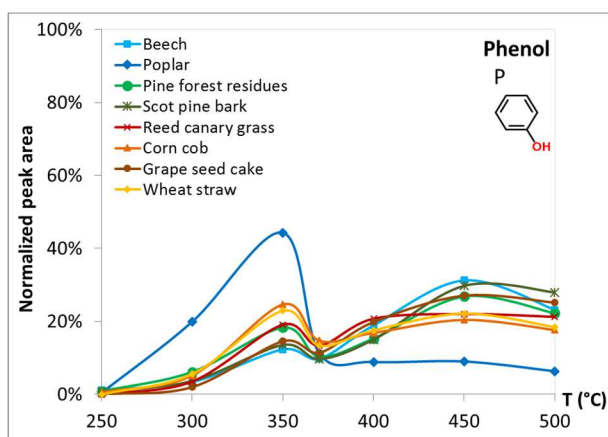
193 reported to acylate the  $\gamma$ -carbon in lignin side chain and ferulic acids polysaccharides. The ferulic acid has  
194 been found to be cross linker forming ether and ester bonds among lignin and carbohydrates, respectively  
195 [16,43]. Similar to hydroxycinnamic acids, acetic acid and phenol formed from hydroxybenzoic acid in poplar  
196 were released in the low temperature region, which reveals that ester bonds are thermally more labile than  
197 ether bonds. The release of carbohydrate derivatives (ketones, furans and sugars) slightly varied among  
198 agricultural biomasses, indicating differences among macromolecular components. The production of volatile  
199 species from grape seed cake is distinct from that of the other agricultural biomasses, which might be due to  
200 its noticeably high lignin content, as well as differences in lignin units. However, similarities were found among  
201 coniferous woods, which are enriched with guaiacyl type lignin, the lignin type also predominant in grape seed  
202 cake.

### 203 **3.2. DETAILED ANALYSIS OF VOLATILE SPECIES PER DETECTED CHEMICAL COMPOUND**

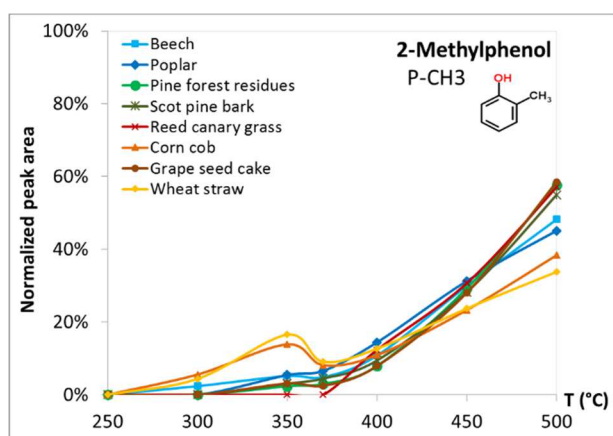
204 Volatile species detected in each fractionated Py-GC/MS experiment were classified in chemical families in  
205 function of their nature into phenolic, carbohydrate and protein derivatives. The production profiles of each  
206 volatile species, represented by the normalized peak area in function of the step of the fractionated pyrolysis,  
207 were compared for the eight biomasses (Figures 2 to 10).

#### 208 **3.2.1. Phenolic derivatives**

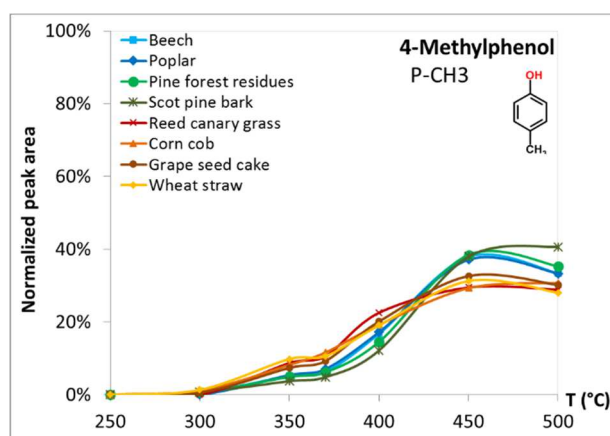
209 Phenol production (Figure 2) occurred in the whole fractionated pyrolysis range and was characterized by two  
210 relative maxima, except for poplar, with a single maximum at 350 °C, representing half of its phenol production.  
211 Poplar contains lignin linked *p*-hydroxybenzoic acid that in pyrolysis is converted to simple phenol..  
212 Methylphenols were characterized by an enhanced production with pyrolysis temperature, with a minor  
213 maximum at 350 °C. It has been reported in the literature that phenols released in the temperature range of  
214 400-600 °C might be produced in secondary reactions from lignin, via demethoxylation of guaiacyl type lignin  
215 derivatives [44]. Phenolic derivatives were released at significantly higher temperatures compared to the  
216 corresponding guaiacyl and syringyl counterparts, which might confirm the secondary reaction phenomenon.  
217 However, by using an optimized duration for each temperature step of the fractionated Py-GC/MS, the yield of  
218 volatile species is expected to be maximized and secondary reactions are expected to be minimized [34].  
219 Therefore the origin of these *p*-hydroxyphenyl derivatives could be mainly attributed to H-type lignin units.  
220 Other minor routes of formation might also be involved, as for phenol, 2-methylphenol and 4-methylphenol,  
221 which can be produced from lignin or the aminoacid tyrosine in proteins [45].



222



223



224 **Figure 2. Profiles of production of phenyl- derivatives of eight biomasses in fractionated Py-GC/MS**

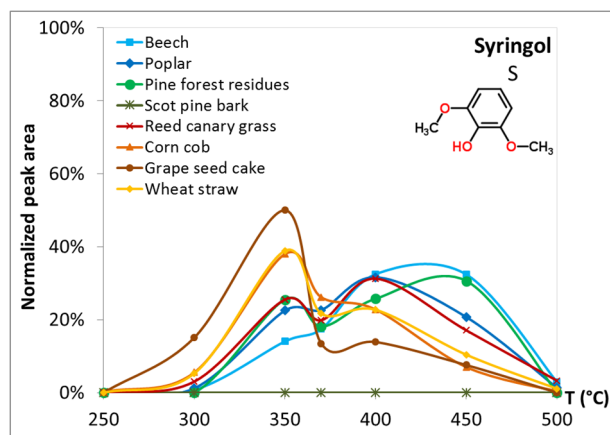
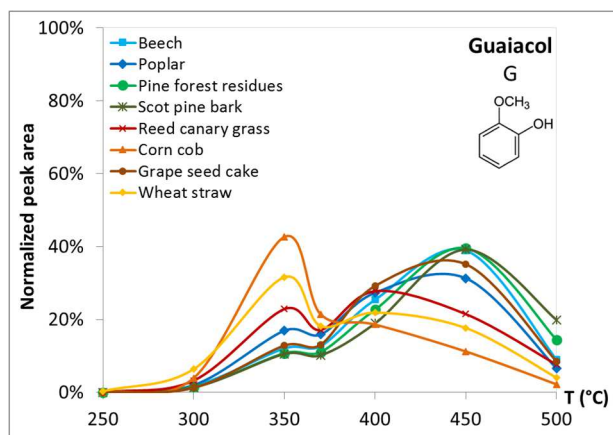
225 Equivalent guaiacyl- and syringyl- derived structures with the same side chain length were compared so as to  
 226 assess if the production routes of phenolic compounds with similar structure might be close (Figures 3 and 4).

227 For guaiacyl- and syringyl- compounds with short side chains (Figure 3), the maximum of production is between  
 228 350 and 370°C for agricultural biomasses (wheat straw and corn cob) and around 450 °C for woody biomasses  
 229 (beech, poplar, forest residues, pine bark). The exception of this behaviour is for 4-methylguaiacol and 4-  
 230 methylsyringol, which present the maximum of production for all biomasses at around 400 to 450 °C. The  
 231 appearance of several maxima in the production profile of 4-methylguaiacol and 4-methylsyringol in  
 232 comparison to the other linear saturated side chain structures indicates that these degradation products might  
 233 be formed from different routes [46].

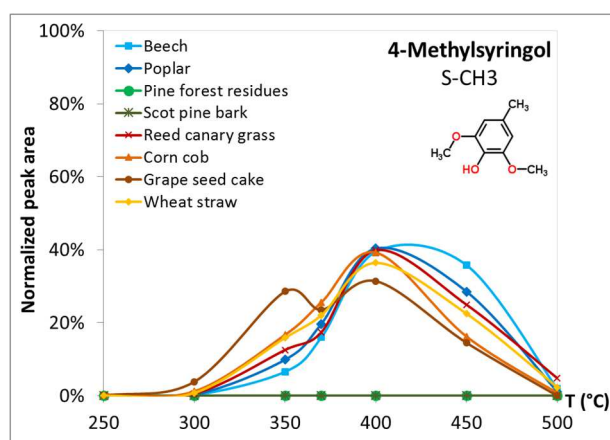
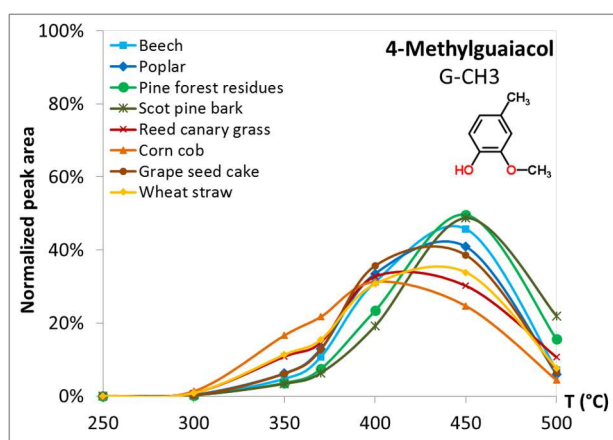
234 By comparing biomass behaviour per families, similarities could be observed for woody biomasses, which  
 235 showed production maxima mainly from 400 to 450 °C (Figure 3). On the contrary, the production of these  
 236 compounds by corn cob and wheat straw occurred in the whole fractionated pyrolysis temperature range, with  
 237 a production maximum from 300 to 400 °C depending on the product. Reed canary grass exhibited an  
 238 intermediate behaviour between woody and agricultural biomasses. Grape seed cake showed a particular  
 239 behaviour which does not correspond between equivalent guaiacyl- and syringyl- derivatives. Indeed, while  
 240 the maximum of its guaiacol production profile is at around 450°C, the corresponding maximum for the syringol  
 241 production is at around 350°C. Concerning methyl- and ethyl- guaiacyl- derivatives, grape seed cake behaviour  
 242 is closer to that of woods, which is not the case for the equivalent syringyl derivatives. Furthermore, only few

243 syringyl type degradation products were detected, whose thermal behaviour was different in comparison to the  
244 corresponding guaiacyl derivatives.

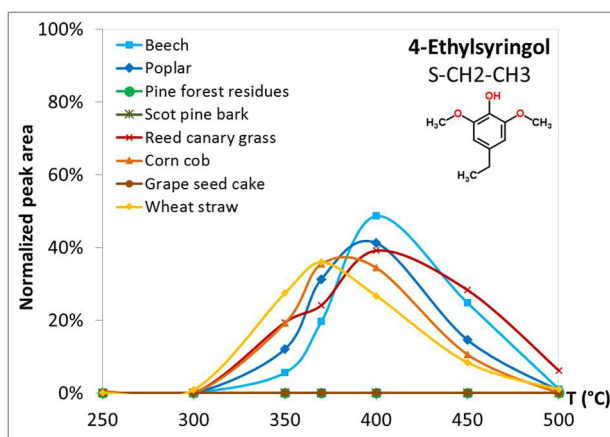
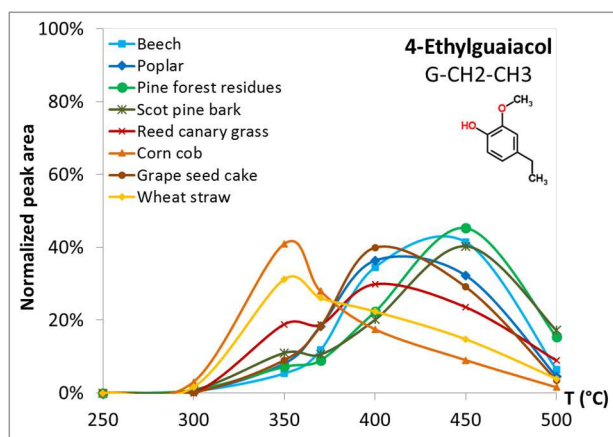
245



246



247



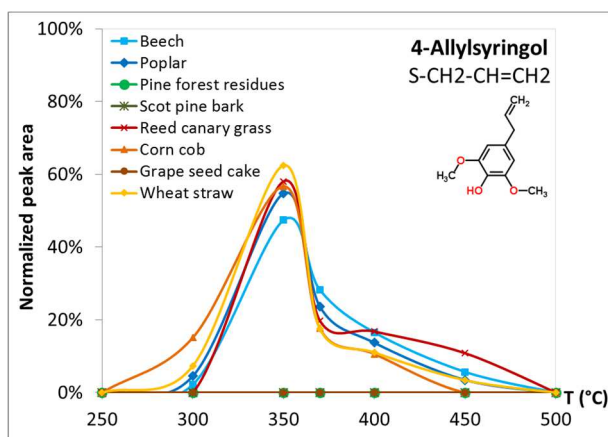
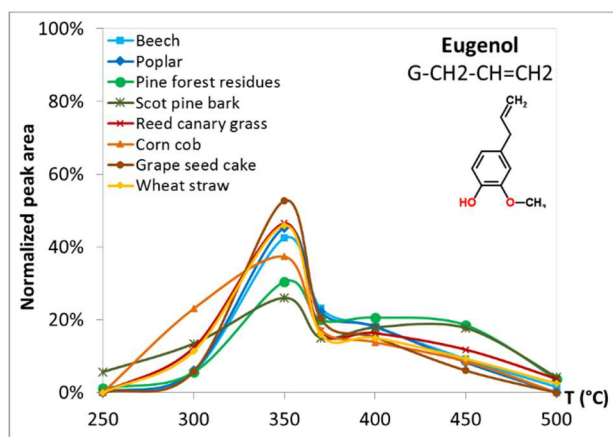
248 **Figure 3. Profiles of production of analogous short chain guaiacyl- (left) and syringyl-(right) derivatives**  
249 **of eight biomasses in fractionated Py-GC/MS**

250 In the case of guaiacyl- and syringyl- compounds with unsaturated and/or oxygenated side-chains (Figure 4),  
251 the maximum of their production was generally at lower temperatures, around 350 °C, for all biomasses. This  
252 maximum was especially marked for grape seed cake, which presented a high lignin content, and reed canary  
253 grass. The formation of all of these compounds continued at higher temperatures, but the yield was much  
254 lower. A second local maximum at higher temperature (around 400 °C) could be observed for the production  
255 of both guaiacyl- and syringyl compounds from all biomasses, indicating a probable different origin for the

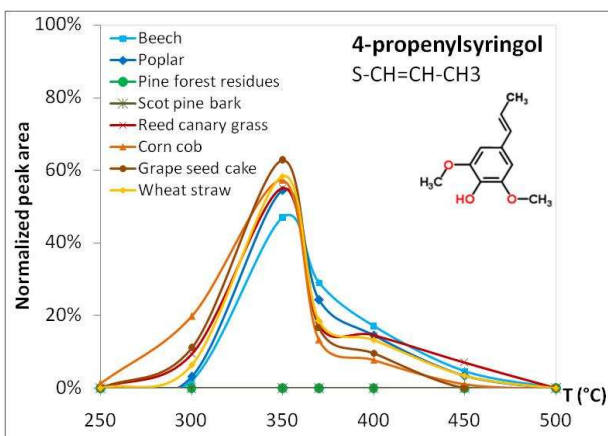
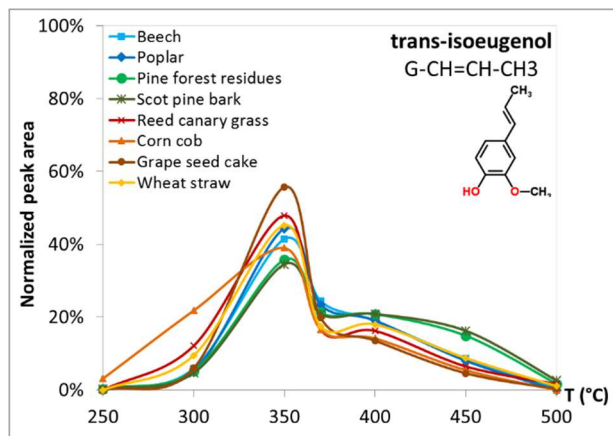
256 same degradation products.

257 The patterns observed for the formation of most of the degradation products in Figure 4 were very similar for  
258 all biomasses, for both the G- and S-series. This may indicate that these products are directly originated from  
259 lignin, as a result of the cleavage of  $\beta$ -O-4 linkage of lignin [44]. Surprising behaviour could be noticed in the  
260 case of vanillin, acetoguaiacone and transconiferyl alcohol (only in the G-series) for corn cob, reed canary  
261 grass and wheat straw. This was probably caused by one or several unknown parallel degradation routes.  
262 Dihydroconiferyl alcohol was released in a significantly high amount already at 300°C from pine forest residue  
263 and scot pine bark. The formation of this compound at low temperatures might be related to the high extractive  
264 content of these biomasses. This hypothesis is supported by the fact that this alcohol has been detected in the  
265 monomer form in coniferous wood extractives [47].

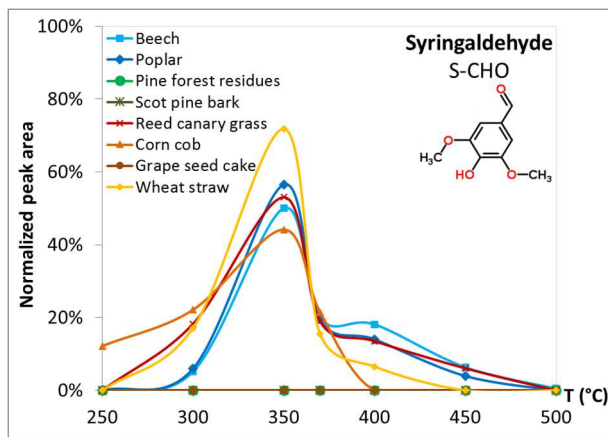
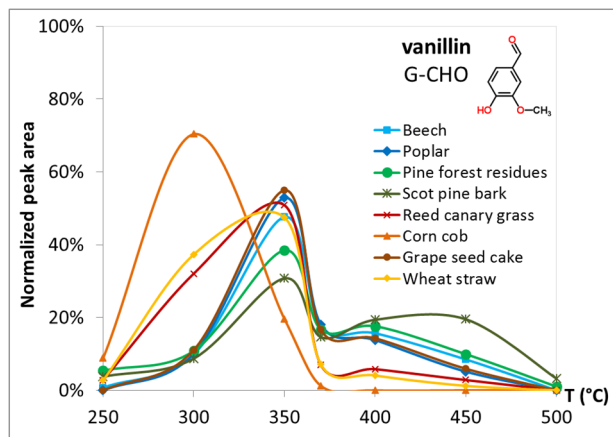
266



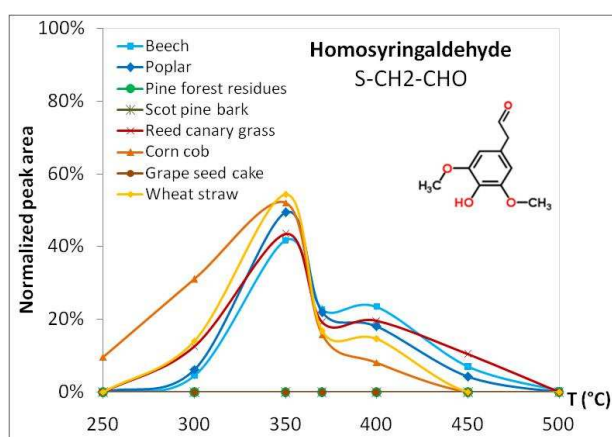
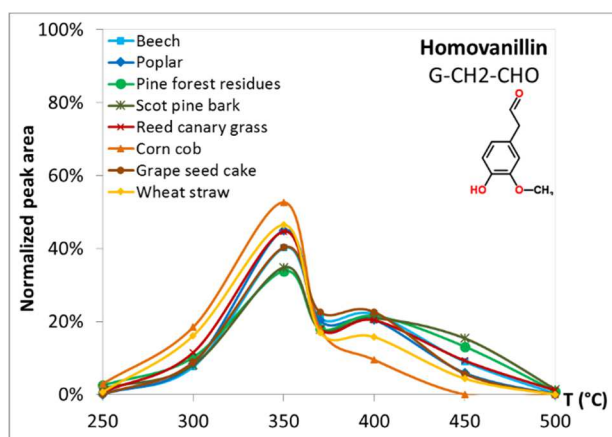
267



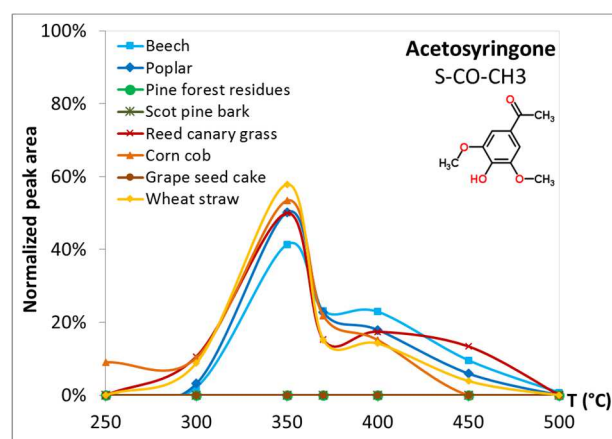
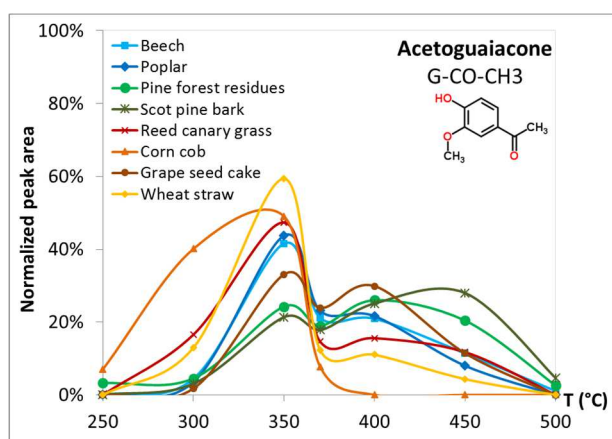
268



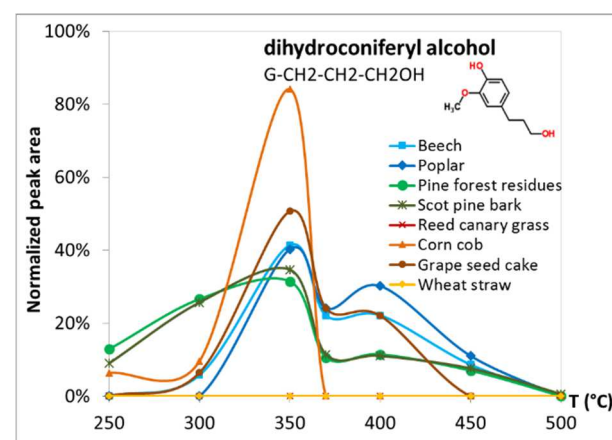
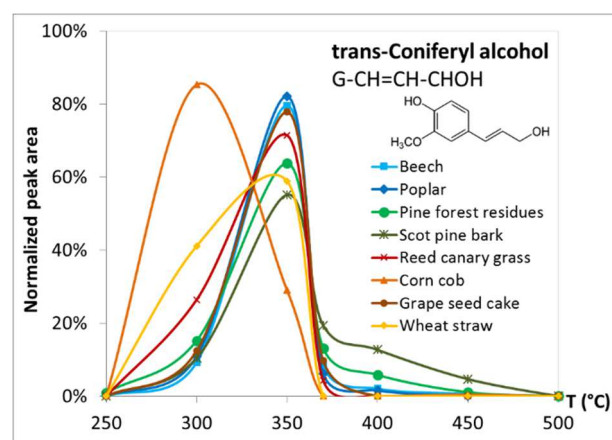
269



270



271

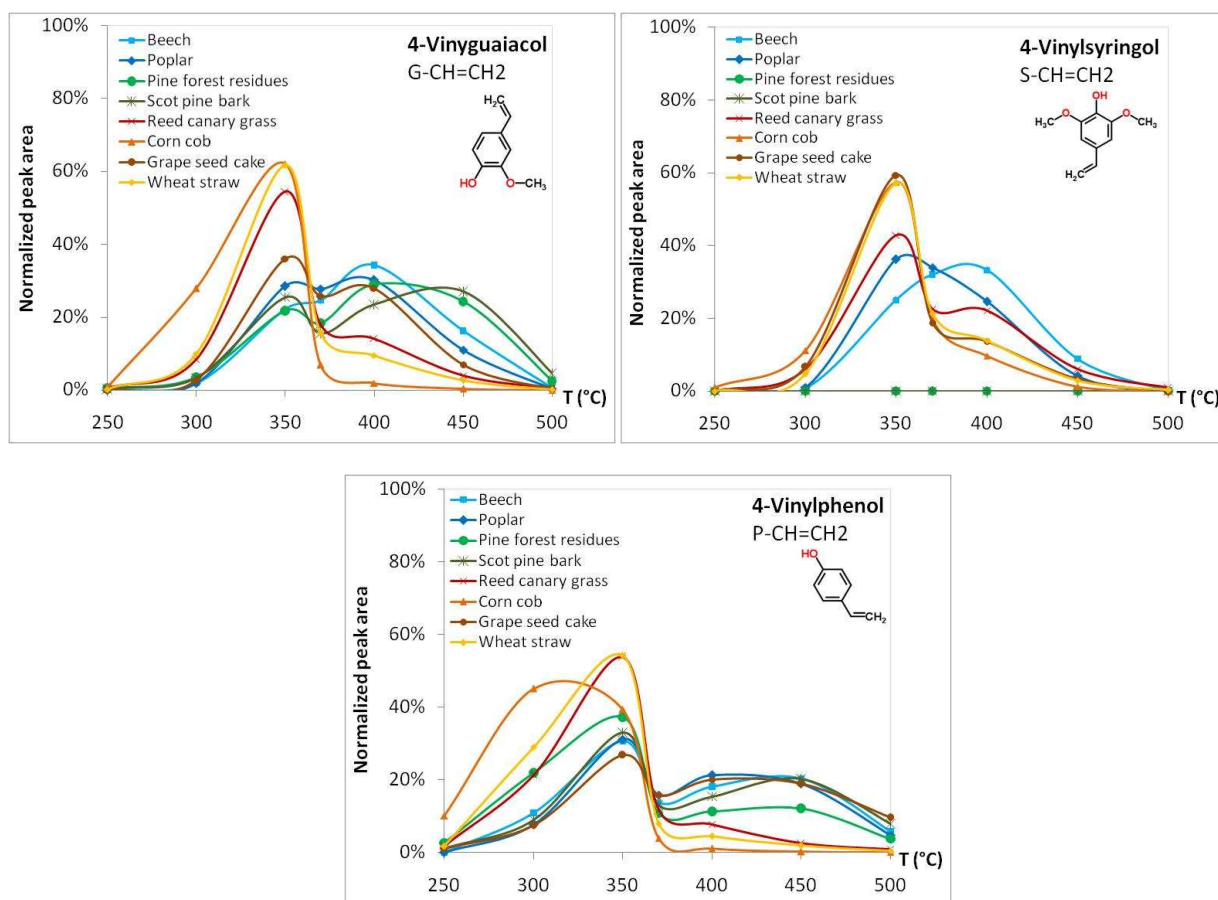


272 **Figure 4. Profiles of production of unsaturated and oxygenated guaiacyl- (left) and syringyl-(right)**  
 273 **derivatives of eight biomasses in fractionated Py-GC/MS**

274 For herbaceous and agricultural biomasses, vinylphenol and vinylguaiacol can be also formed from *p*-  
 275 hydroxycinnamic acids (*p*-coumaric and ferulic acids) in addition to lignin [15,48]. According to [34], the first  
 276 maximum of production of these compounds could correspond to the production from *p*-hydroxycinnamic  
 277 acids, while the maximum at higher temperatures could represent the formation of this compound from lignin.  
 278 In the case of wheat straw, corn cob and reed canary grass, the maximum of the production for 4-vinylguaiacol  
 279 was at around 350 °C, which could indicate that the major part of the production of this compound is derived  
 280 from *p*-hydroxycinnamic acids. In the case of woody biomasses, the maximum was at intermediate and higher  
 281 temperatures. For grape seed cake (high content in lignin) and reed canary grass (herbaceous crop), the

282 behaviour was intermediate (Figure 5).

283



284

285 **Figure 5. Profiles of production of vinyl derivatives of eight biomasses in fractionated Py-GC/MS**

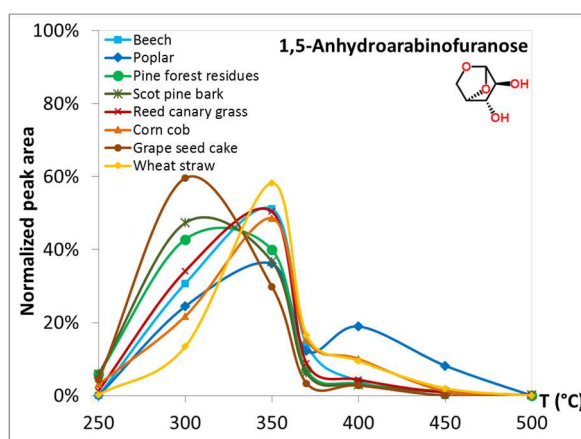
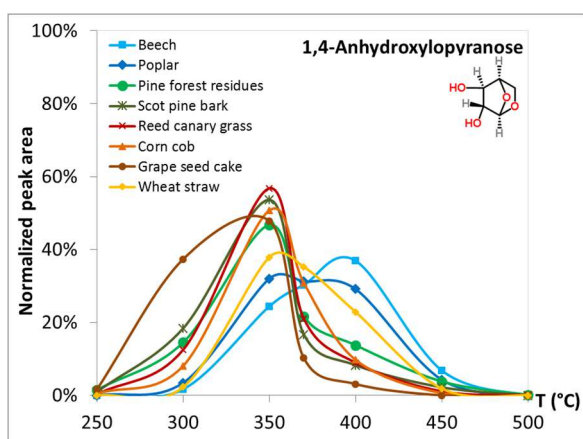
286

### 3.2.2. Carbohydrate derivatives

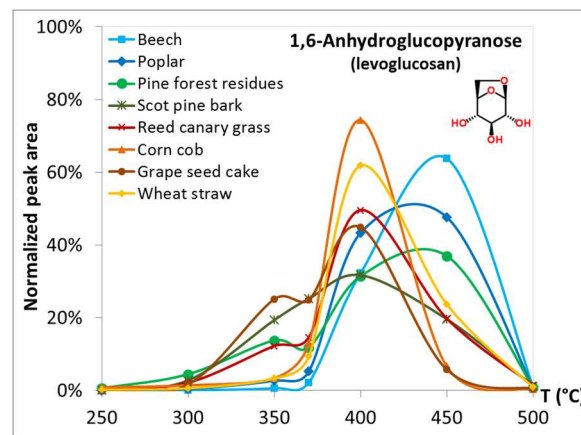
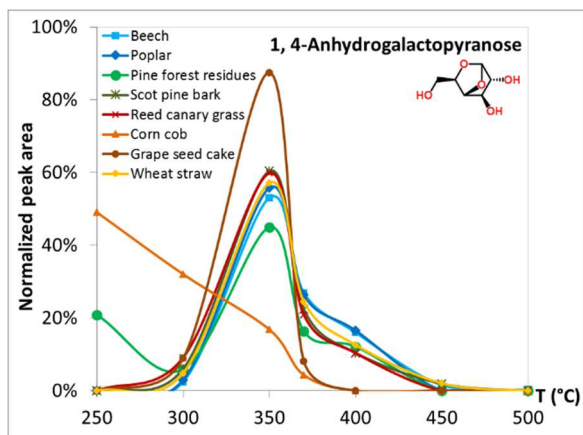
287 Six carbohydrate-derived molecules were identified in the volatile mixture resulting from the Py-GC/MS  
288 experiments of 8 biomasses (Figure 6). The production of these molecules was reported to be directly related  
289 to the thermal decomposition of cellulose and hemicelluloses in biomass [45,49]. Hemicelluloses are an  
290 amorphous heteropolymer, which is thermally decomposed at low pyrolysis temperatures (250 to 320 °C)  
291 [50,51]. Cellulose is a more crystalline polymer that degrades at slightly higher temperatures (around 280 to  
292 400 °C) [51–53]. The origin of the sugar molecules released can therefore be associated to their origin in  
293 function of their maximum temperature of production. As a result, hemicelluloses derivatives would be 1,4-  
294 anhydroxylopyranose and 1,5-anhydro-4-deoxypent-1-en-ulose (derived from xylan), 1,5-  
295 anhydroarabinofuranose (derived from arabinan) [23], 1,4-anhydrogalactopyranose (derived from galactan),  
296 since their maximum temperature of production was between 300 and 350 °C, which corresponds to the  
297 temperature range of hemicelluloses degradation. On the contrary, 1,6-anhydroglucopyranose (levoglucosan)  
298 would be derived from cellulose, as its maximum of production was at around 400 °C for annual plants and  
299 450 °C for woods. Finally, the production profile of 1,4-dideoxy-D-glycero-hex-1-enopyranos-3-ulose occurred  
300 at lower temperatures for grape seed cake and softwood (350 °C), and at higher temperatures for agricultural  
301 biomass, herbaceous crops and hardwood. This compound is formed from cellulose- and hexose-sugar-based

302 hemicelluloses, such as galactoglucomannan and glucomannan. Its profile of production, compared to those  
 303 of 1,4-galactopyranose and 1,6-anhydroglucopyranose, suggests that the first maximum would mainly  
 304 correspond to the degradation of hexose-sugar-based hemicelluloses and the second maximum could be  
 305 attributable to cellulose. This behaviour might be in agreement with biomass sugar composition (Table 2), as  
 306 a higher mannose and galactose content was measured for grape seed cake and softwood, including bark ,  
 307 while the cellulose content is higher for deciduous wood and agricultural biomasses (38.1 to 42.7 %, compared  
 308 to 7.8 to 22.3 %).

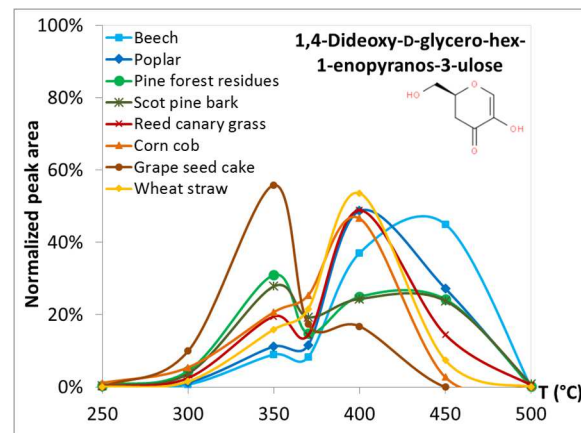
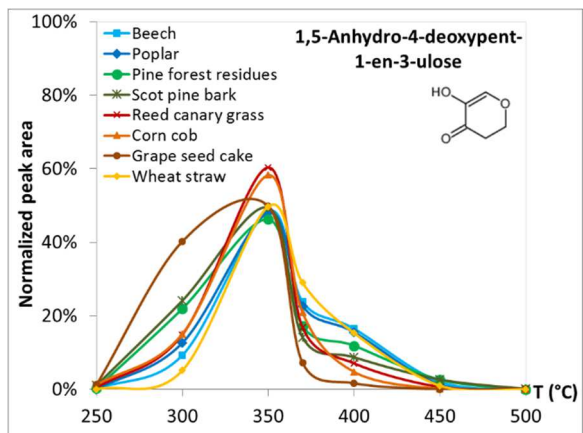
309



310



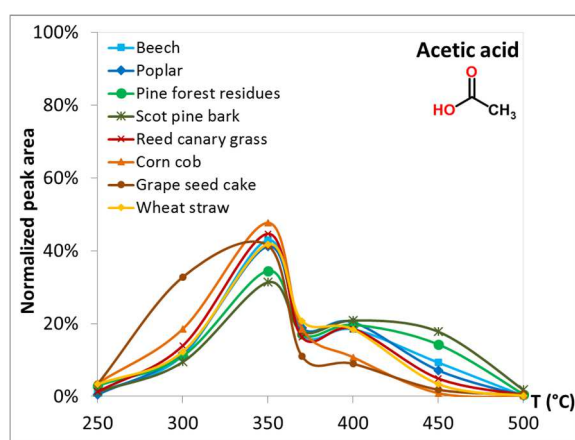
311



312 **Figure 6. Profiles of production of sugar molecules of eight biomasses in fractionated Py-GC/MS**

313 Small molecules, including acids, ketones and furans, are principally carbohydrate derivatives. Acetic acid is  
 314 one of the major detected compounds in fractionated Py-GC/MS of biomass (Figure 7). Its profile of formation,

315 similar for all the biomasses in this study, is characterized by a maximum of production at 350 °C, followed by  
316 a regular production until 450 °C. The main mechanism of formation of acetic acid is from the scission of acetyl  
317 groups in hemicelluloses [54], which is accordance with the maximum of production at lower temperatures in  
318 Py-GC/MS. In addition to hemicelluloses, in some herbaceous plants the  $\gamma$ -carbon in lignin side chain has been  
319 reported to be acetylated and is susceptible to release acetic acid [15]. However, this release of acetic acid  
320 from lignin side chain is expected to occur in the same temperature region as from hemicelluloses, due to the  
321 ester linkage, but in a lower amount. Other mechanisms have been proposed, as the decomposition of uronic  
322 acid unit in hemicelluloses and through the complex reaction of ring-opened sugar units [55,56], which could  
323 correspond to the regular production at intermediate temperatures in Py-GC/MS. The differences in acetyl  
324 content in the biomasses studied (from 1.6 to 8.3 %) do not allow to distinguish a higher production of acetic  
325 acid in Figure 7, as the percentages of the total production per pyrolysis step are represented.

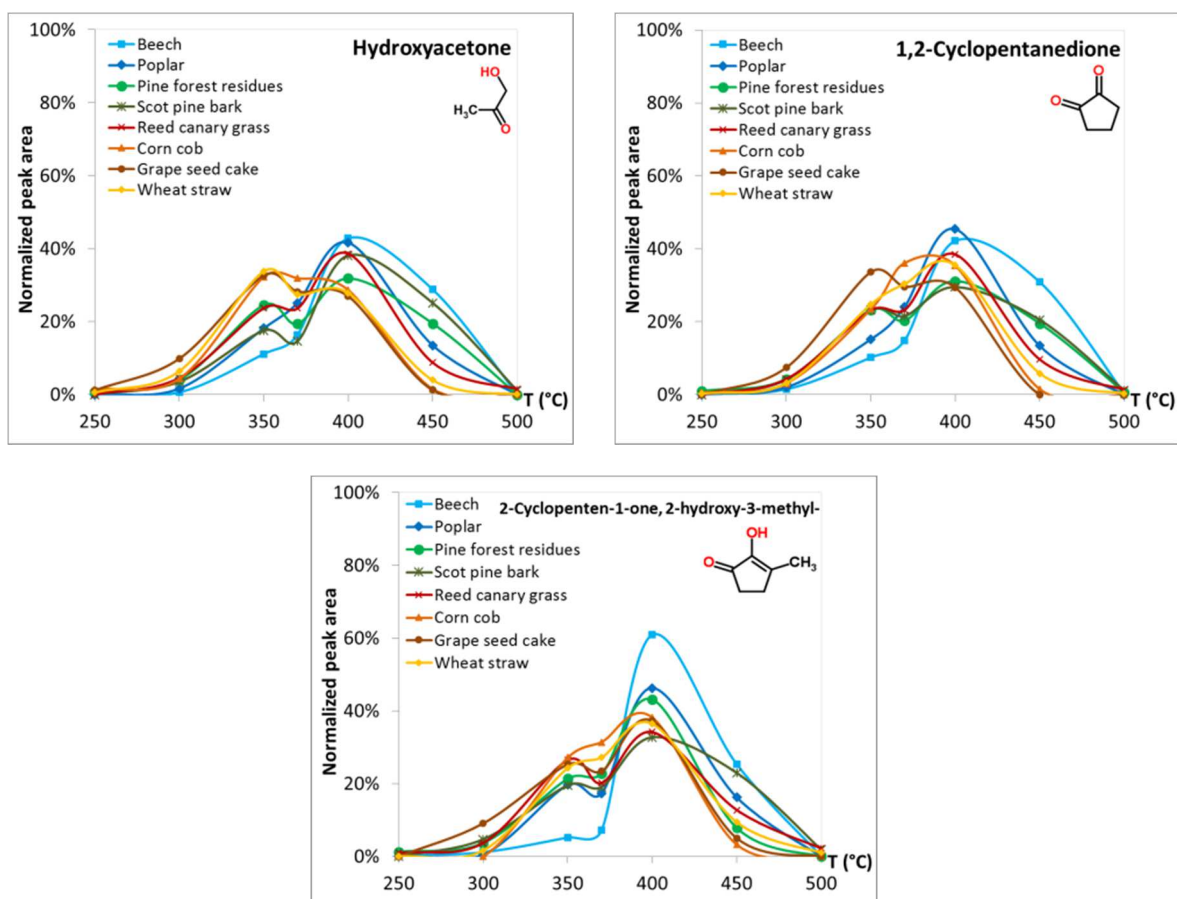


326

327 **Figure 7. Profile of production of acetic acid of eight biomasses in fractionated Py-GC/MS**

328 One linear ketone (hydroxyacetone) and two cyclic ketones (1,2-cyclopentanedione and 2-cyclopenten-1-one,  
329 2-hydroxy-3-methyl-) were identified in the experiments (Figure 8). Ketones and other small compounds were  
330 reported to be released in the rapid depolymerization of hemicelluloses, but also from cellulose [57], directly  
331 or through unstable intermediaries which go through dehydration, fragmentation and secondary reactions [58].  
332 Cyclic ketones are produced in hemicelluloses depolymerization [5,59,60], derived from pyran or furan rings  
333 [58], but also in cellulose pyrolysis at high temperatures [57,61,62]. These pathways of formation might be in  
334 accordance with the highest percentage of production at the intermediate steps of the fractionated pyrolysis,  
335 without any clearly observable maximum temperature. Noteworthy is the exception of beech, which exhibited  
336 increasing production until 400 °C, suggesting the presence of some parallel formation routes of this  
337 degradation product in this biomass.

338

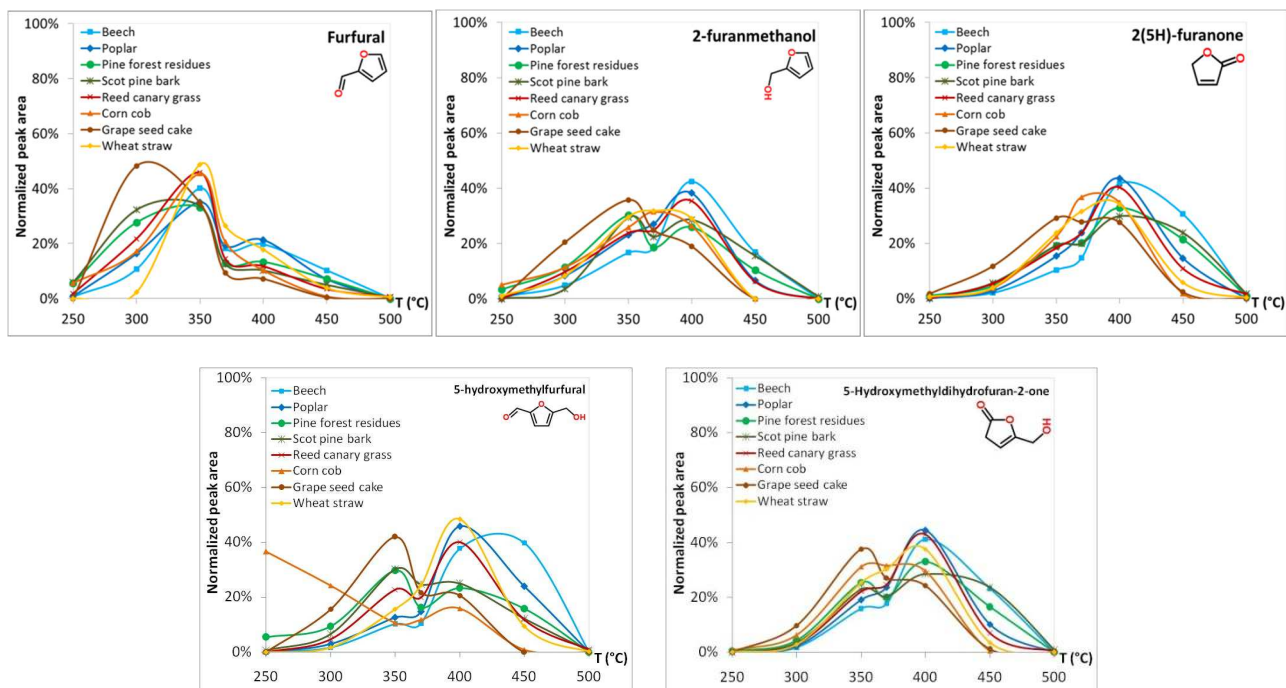


339

340 **Figure 8. Profiles of production of ketones of eight biomasses in fractionated Py-GC/MS**

341 Furans were in general produced at intermediate to high temperatures under the established Py-GC/MS  
 342 operating conditions (Figure 9). Furfural constituted an exception, since it was produced mainly around 350  
 343 °C, with a small peak at 400 °C. The origin of furans in the thermal decomposition of cellulose was pointed out  
 344 as depolymerization reactions. They consist in a contraction of the pyran ring of levoglucosan through the  
 345 elimination of oxygenated groups and the formation of double bonds (C=C) could end in a furan ring in cellulose  
 346 char. Then, weak bonds might break and liberate furan compounds such as furfural [63]. The release of furfural  
 347 from hemicelluloses is attributed to the ring-opening and rearrangement reactions of the xylan unit [59], which  
 348 might occur at lower temperatures than the formation of this product from cellulose. In general, furan production  
 349 from hemicelluloses is related to depolymerization reactions occurring by cleavage of glycosidic linkages  
 350 between sugar units. This formation typically happens at temperatures slightly higher for glucomannan-based  
 351 hemicelluloses, compared to xylan-based hemicelluloses [60], as pyran rings derived from glucomannan (6  
 352 C-atoms) can change into more stable furan rings (5 C-atoms) [58]. The two relative maxima observed in the  
 353 production curves of furans might contribute to explain the percentage of the production of each pyrolysis  
 354 compound derived from hemicelluloses or from cellulose, respectively, as hemicelluloses thermal degradation  
 355 starts at lower temperatures. Most of the furfural production may be derived from hemicelluloses, as the  
 356 maximum of the curve is at around 350 °C, or even at lower temperature for grape seed cake and coniferous  
 357 wood. Deciduous wood and reed canary grass showed a maximum of production at around 400 °C for the  
 358 other furans detected. They might therefore come from cellulose, or from hemicelluloses [64], either less  
 359 accessible or linked to cellulose.

360



361

362 **Figure 9. Profiles of production of furans of eight biomasses in fractionated Py-GC/MS**

363

### 3.2.3. Protein derivatives

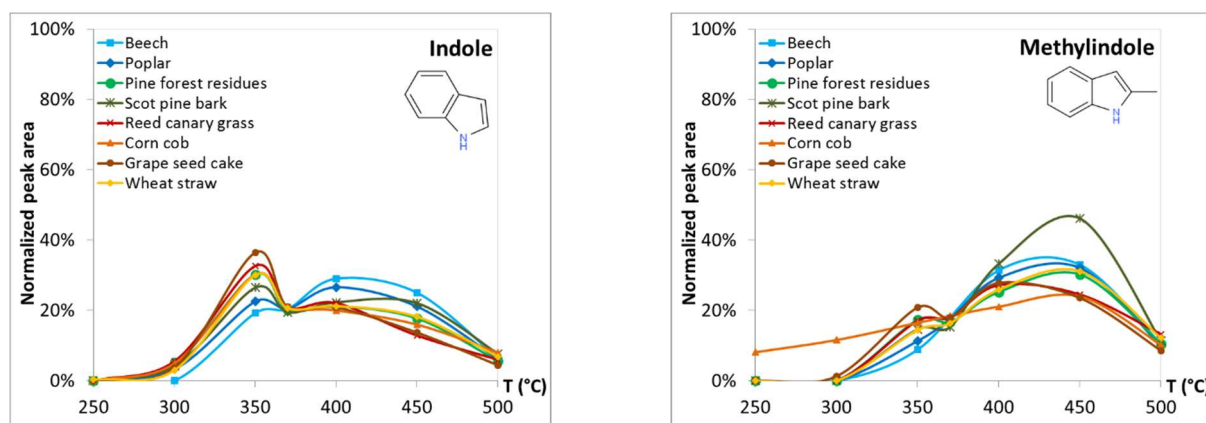
364

365 Indole and methylindole, which were reported to be derived from protein thermal degradation [57,58], are  
366 produced in the whole range of fractionated pyrolysis (Figure 10). Their production profiles are different from  
367 those of phenol, 2-methylphenol and 4-methylphenol, which were reported to be partially produced by proteins  
[45]. This confirms that these phenol derivatives have also other sources than proteins.

368

369 The fact that the specific marker compounds (the indoles) for proteins were detected in all biomasses is an  
370 indication of the high sensitivity of the applied analysis method, as the protein content is extremely low,  
especially in the woody biomasses.

371



372 **Figure 10. Profiles of production of protein derivatives of eight biomasses in fractionated Py-GC/MS**

373

## 4. CONCLUSIONS

374

Fractionated pyrolysis coupled to GC/MS was shown as a useful tool to distinguish the origin of the pyrolysis

375 volatile products from the macromolecular components of biomass, namely cellulose, hemicelluloses and  
376 lignin. Important differences could be observed in the distribution of the pyrolysis volatile products in function  
377 of the biomass type. In particular, deciduous wood, represented by beech and poplar, exhibited similar  
378 behaviours in terms of volatile species release. This was also showed for coniferous wood, represented by  
379 pine forest residues and Scot pine bark. On the contrary, agricultural biomasses showed strong differences in  
380 the distribution of the pyrolysis products along the temperature/duration pyrolysis program. These differences  
381 may be due to the more heterogeneous macromolecular composition of agricultural biomasses, particularly  
382 noticeable between corn cob, which presents a high polysaccharide content, and grape seed cake, with a high  
383 lignin content.

384 The percentages of each pyrolysis product produced per temperature/duration step of the pyrolysis program,  
385 compared to the total production of the volatile species, were shown to contribute to distinguish the origin of  
386 the pyrolysis products from cellulose, hemicelluloses and lignin. In the case of phenyl derivatives, guaiacyls  
387 and syringyls with longer side chain substituents were produced at lower pyrolysis temperatures, while  
388 phenolic compounds without side chain, such as guaiacol and syringol, were released at higher temperatures.  
389 This indicates a more difficult removal of these last compounds from the biomass structure in thermal  
390 degradation, compared to the long-chain phenolic compounds that are expected to be released from easily  
391 cleaved aryl ether structures. Furthermore, the structure of hardwood and softwood might be more resistant  
392 to thermal degradation, compared to agricultural biomasses, according to the production profiles of lignin  
393 derivatives. In the case of polysaccharides, pyrolysis products exhibiting a maximum in the production profile  
394 at low to intermediate pyrolysis temperatures (around 350 °C) might be mainly derived from hemicelluloses.  
395 On the contrary, those presenting a maximum at intermediate to high pyrolysis temperatures (around 400 °C)  
396 would be derived from cellulose or from less accessible hemicelluloses.

## 397 **5. ACKNOWLEDGMENTS**

398 This project has received funding from the European Union's Horizon 2020 research and innovation program  
399 under grant agreement No 637020–MOBILE FLIP. The Université Fédérale de Toulouse Midi-Pyrénées  
400 (France), CEA Grenoble (France) and VTT Finland are also acknowledged for the support of this work.

## 401 **6. REFERENCES**

- 402 [1] European Commission, State of play on the sustainability of solid and gaseous biomass used for  
403 electricity, heating and cooling in the EU, 2014.  
404 [https://ec.europa.eu/energy/sites/ener/files/2014\\_biomass\\_state\\_of\\_play\\_.pdf](https://ec.europa.eu/energy/sites/ener/files/2014_biomass_state_of_play_.pdf) (accessed September 28,  
405 2016).
- 406 [2] P.F.H. Harmsen, W.J.J. Huijgen, L.M. Bermúdez López, R.R.C. Bakker, Literature Review of Physical  
407 and Chemical Pretreatment Processes for Lignocellulosic Biomass, Energy Research Centre of the  
408 Netherlands, 2010.
- 409 [3] S.V. Pisupati, A.H. Tchapda, Chapter 15: Thermochemical Processing of biomass, in: Adv. Bioprocess  
410 Technol., Pogaku Ravindra, Switzerland, 2015.
- 411 [4] T. Hosoya, H. Kawamoto, S. Saka, Cellulose–hemicellulose and cellulose–lignin interactions in wood  
412 pyrolysis at gasification temperature, *J. Anal. Appl. Pyrolysis*. 80 (2007) 118–125.  
413 doi:10.1016/j.jaap.2007.01.006.

- 414 [5] S.D. Stefanidis, K.G. Kalogiannis, E.F. Iliopoulou, C.M. Michailof, P.A. Pilavachi, A.A. Lappas, A  
415 study of lignocellulosic biomass pyrolysis via the pyrolysis of cellulose, hemicellulose and lignin, *J.*  
416 *Anal. Appl. Pyrolysis.* 105 (2014) 143–150. doi:10.1016/j.jaap.2013.10.013.
- 417 [6] T. Kan, V. Strezov, T.J. Evans, Lignocellulosic biomass pyrolysis: A review of product properties and  
418 effects of pyrolysis parameters, *Renew. Sustain. Energy Rev.* 57 (2016) 1126–1140.  
419 doi:10.1016/j.rser.2015.12.185.
- 420 [7] S.K. Guha, H. Kobayashi, A. Fukuoka, Chapter 13: Conversion of cellulose to sugar, in: Chapter  
421 13 Conversion Cellul. Sugars, 2010. [http://pubs.rsc.org/en/content/chapter/bk9781849730358-](http://pubs.rsc.org/en/content/chapter/bk9781849730358-00344/978-1-84973-035-8)  
422 [00344/978-1-84973-035-8](http://pubs.rsc.org/en/content/chapter/bk9781849730358-00344/978-1-84973-035-8) (accessed March 24, 2016).
- 423 [8] A. Dufresne, *Les nanotechnologies dans l'industrie papetière*, Tech. Ing. (2010).
- 424 [9] L.D. Gomez, C.G. Steele-King, S.J. McQueen-Mason, Sustainable liquid biofuels from biomass: the  
425 writing's on the walls, *New Phytol.* 178 (2008) 473–485. doi:10.1111/j.1469-8137.2008.02422.x.
- 426 [10] H.V. Scheller, P. Ulvskov, Hemicelluloses, *Annu. Rev. Plant Biol.* 61 (2010) 263–289.  
427 doi:10.1146/annurev-arplant-042809-112315.
- 428 [11] B. Monties, *Les polymères végétaux: les lignines*, 1980.
- 429 [12] Kirk-Othmer, *Encyclopedia of Chemical Technology*, Wiley, 1999.  
430 <http://onlinelibrary.wiley.com/book/10.1002/0471238961/homepage/EditorsContributors.html>  
431 (accessed March 22, 2016).
- 432 [13] K. Morreel, J. Ralph, H. Kim, F. Lu, G. Goeminne, S. Ralph, E. Messens, W. Boerjan, Profiling of  
433 Oligolignols Reveals Monolignol Coupling Conditions in Lignifying Poplar Xylem, *Plant Physiol.* 136  
434 (2004) 3537–3549. doi:10.1104/pp.104.049304.
- 435 [14] A. Sequeiros, J. Labidi, Characterization and determination of the S/G ratio via Py-GC/MS of agricultural  
436 and industrial residues, *Ind. Crops Prod.* 97 (2017) 469–476. doi:10.1016/j.indcrop.2016.12.056.
- 437 [15] J.C. del Río, A. Gutiérrez, I.M. Rodríguez, D. Ibarra, Á.T. Martínez, Composition of non-woody plant  
438 lignins and cinnamic acids by Py-GC/MS, Py/TMAH and FT-IR, *J. Anal. Appl. Pyrolysis.* 79 (2007) 39–  
439 46. doi:10.1016/j.jaap.2006.09.003.
- 440 [16] J. Ralph, Hydroxycinnamates in lignification, *Phytochem. Rev.* 9 (2010) 65–83. doi:10.1007/s11101-  
441 009-9141-9.
- 442 [17] Y.W. Sari, U. Syafitri, J.P.M. Sanders, M.E. Bruins, How biomass composition determines protein  
443 extractability, *Ind. Crops Prod.* 70 (2015) 125–133. doi:10.1016/j.indcrop.2015.03.020.
- 444 [18] C. Dupont, S. Rougé, A. Berthelot, D. Da Silva Perez, A. Graffin, F. Labalette, C. Laboubée, J.-C.  
445 Mithouard, S. Pitocchi, Bioenergy II: Suitability of Wood Chips and Various Biomass Types for Use in  
446 Plant of BtL Production by Gasification, *Int. J. Chem. React. Eng.* 8 (2010). doi:10.2202/1542-  
447 6580.1949.
- 448 [19] J.J. Harrington, R. Booker, Astley R.J., Modelling the elastic properties of softwood. Part I: The cell-  
449 wall lamellae, *Holz Als Roh- Werkst.* (1998) 37–41.
- 450 [20] E. Sjöström, *Wood chemistry: Fundamentals and Applications*, 2nd ed., Academic Press, 1993.
- 451 [21] USDA, *Wood handbook: wood as an engineering material - US Department of Agriculture*, 2010.
- 452 [22] J.-L. Faulon, G.A. Carlson, P.G. Hatcher, A three-dimensional model for lignocellulose from  
453 gymnospermous wood, *Org. Geochem.* 21 (1994) 1169–1179. doi:10.1016/0146-6380(94)90161-9.
- 454 [23] K. Werner, L. Pommer, M. Broström, Thermal decomposition of hemicelluloses, *J. Anal. Appl.*  
455 *Pyrolysis.* 110 (2014) 130–137. doi:10.1016/j.jaap.2014.08.013.
- 456 [24] J. Vogel, Unique aspects of the grass cell wall, *Curr. Opin. Plant Biol.* 11 (2008) 301–307.  
457 doi:10.1016/j.pbi.2008.03.002.

- 458 [25] M. Mattonai, D. Licursi, C. Antonetti, A.M. Raspolli Galletti, E. Ribechini, Py-GC/MS and HPLC-DAD  
459 characterization of hazelnut shell and cuticle: Insights into possible re-evaluation of waste biomass, *J.*  
460 *Anal. Appl. Pyrolysis.* (2017). doi:10.1016/j.jaap.2017.07.019.
- 461 [26] T. Ohra-aho, F.J.B. Gomes, J.L. Colodette, T. Tamminen, S/G ratio and lignin structure among  
462 *Eucalyptus* hybrids determined by Py-GC/MS and nitrobenzene oxidation, *J. Anal. Appl. Pyrolysis.* 101  
463 (2013) 166–171. doi:10.1016/j.jaap.2013.01.015.
- 464 [27] J. Zhao, W. Xiuwen, J. Hu, Q. Liu, D. Shen, R. Xiao, Thermal degradation of softwood lignin and  
465 hardwood lignin by TG-FTIR and Py-GC/MS, *Polym. Degrad. Stab.* 108 (2014) 133–138.  
466 doi:10.1016/j.polymdegradstab.2014.06.006.
- 467 [28] J. Rencoret, J.C. del Río, K.G.J. Nierop, A. Gutiérrez, J. Ralph, Rapid Py-GC/MS assessment of the  
468 structural alterations of lignins in genetically modified plants, *J. Anal. Appl. Pyrolysis.* 121 (2016) 155–  
469 164. doi:10.1016/j.jaap.2016.07.016.
- 470 [29] L.C.A. Barbosa, C.R.A. Maltha, V.L. Silva, J.L. Colodette, Determination of the syringyl/guaiacyl ratio  
471 in eucalyptus wood by pyrolysis-gas chromatography/mass spectrometry (PY-GC/MS), *Quím. Nova.*  
472 31 (2008) 2035–2041. doi:10.1590/S0100-40422008000800023.
- 473 [30] C.F. Lima, L.C.A. Barbosa, C.R. Marcelo, F.O. Silvério, J.L. Colodette, Comparison between analytical  
474 pyrolysis and nitrobenzene oxidation for determination of syringyl/guaiacyl ratio in *Eucalyptus* spp.  
475 lignin, *BioResources.* 3 (2008) 701–712. doi:10.15376/biores.3.3.701-712.
- 476 [31] L. Chen, X. Wang, H. Yang, Q. Lu, D. Li, Q. Yang, H. Chen, Study on pyrolysis behaviors of non-woody  
477 lignins with TG-FTIR and Py-GC/MS, *J. Anal. Appl. Pyrolysis.* 113 (2015) 499–507.  
478 doi:10.1016/j.jaap.2015.03.018.
- 479 [32] T. Ohra-aho, F.J.B. Gomes, J.L. Colodette, T. Tamminen, Carbohydrate composition in *Eucalyptus* wood  
480 and pulps – Comparison between Py-GC/MS and acid hydrolysis, *J. Anal. Appl. Pyrolysis.* 129 (2018)  
481 215–220. doi:10.1016/j.jaap.2017.11.010.
- 482 [33] A.O. Balogun, O.A. Lasode, A.G. McDonald, Thermochemical and pyrolytic analyses of *Musa* spp.  
483 residues from the rainforest belt of Nigeria, *Environ. Prog. Sustain. Energy.* 37 (2018) 1932–1941.  
484 doi:10.1002/ep.12869.
- 485 [34] M. González Martínez, T. Ohra-aho, D. da Silva Perez, T. Tamminen, C. Dupont, Influence of step  
486 duration in fractionated Py-GC/MS of lignocellulosic biomass, *J. Anal. Appl. Pyrolysis.* 137 (2019) 195–  
487 202. doi:10.1016/j.jaap.2018.11.026.
- 488 [35] P.R. Patwardhan, J.A. Satrio, R.C. Brown, B.H. Shanks, Influence of inorganic salts on the primary  
489 pyrolysis products of cellulose, *Bioresour. Technol.* 101 (2010) 4646–4655.  
490 doi:10.1016/j.biortech.2010.01.112.
- 491 [36] M. Kleen, G. Gellerstedt, Influence of inorganic species on the formation of polysaccharide and lignin  
492 degradation products in the analytical pyrolysis of pulps, *J. Anal. Appl. Pyrolysis.* 35 (1995) 15–41.  
493 doi:10.1016/0165-2370(95)00893-J.
- 494 [37] S. Jacob, D. Da Silva Perez, C. Dupont, J.-M. Commandré, F. Broust, A. Carriau, D. Sacco, Short rotation  
495 forestry feedstock: Influence of particle size segregation on biomass properties, *Fuel.* 111 (2013) 820–  
496 828. doi:10.1016/j.fuel.2013.04.043.
- 497 [38] M. González Martínez, C. Dupont, S. Thiéry, X.-M. Meyer, C. Gourdon, Impact of biomass diversity on  
498 torrefaction: Study of solid conversion and volatile species formation through an innovative TGA-  
499 GC/MS apparatus, *Biomass Bioenergy.* 119 (2018) 43–53. doi:10.1016/j.biombioe.2018.09.002.
- 500 [39] O. Faix, D. Meier, I. Fortlann, Thermal degradation products of wood. Gas chromatographic separation  
501 and mass spectrometric characterization of lignin derived products, *Holz Als Roh- Werkst.* (1990) 281–  
502 285.
- 503 [40] O. Faix, D. Meier, I. Fortlann, Thermal degradation products of wood. A collection of electron-impact  
504 (EI) mass spectra of monomeric lignin derived products, *Holz Als Roh- Werkst.* (1990) 351–354.

- 505 [41] O. Faix, I. Fortlann, J. Bremer, D. Meier, Thermal degradation products of wood. Gas chromatographic  
506 separation and mass spectrometric characterization of polysaccharide derived products, *Holz Als Roh-*  
507 *Werkst.* (1991) 213–219.
- 508 [42] O. Faix, D. Meier, I. Fortlann, J. Bremer, Thermal degradation products of wood. A collection of  
509 electron-impact (EI) mass spectra of monomeric polysaccharide derived products, *Holz Als Roh- Werkst.*  
510 (1991) 299–304.
- 511 [43] C. Crestini, D.S. Argyropoulos, Structural Analysis of Wheat Straw Lignin by Quantitative 31P and 2D  
512 NMR Spectroscopy. The Occurrence of Ester Bonds and  $\alpha$ -O-4 Substructures, *J. Agric. Food Chem.* 45  
513 (1997) 1212–1219. doi:10.1021/jf960568k.
- 514 [44] H. Kawamoto, Lignin pyrolysis reactions, *J. Wood Sci.* 63 (2017) 117–132. doi:10.1007/s10086-016-  
515 1606-z.
- 516 [45] G.C. Galletti, P. Bocchini, Pyrolysis/gas chromatography/mass spectrometry of lignocellulose, *Rapid*  
517 *Commun. Mass Spectrom.* 9 (1995) 815–826. doi:10.1002/rcm.1290090920.
- 518 [46] K. Kuroda, A. Nakagawa-izumi, Analytical pyrolysis of lignin: Products stemming from  $\beta$ -5  
519 substructures, *Org. Geochem.* 37 (2006) 665–673. doi:10.1016/j.orggeochem.2006.01.012.
- 520 [47] D. Fengel, G. Wegener, W. De Gruyer, *Wood—chemistry, ultrastructure, reactions*, Berlin and New  
521 York, 1984.
- 522 [48] T.B.T. Lam, K. Kadoya, K. Iiyama, Bonding of hydroxycinnamic acids to lignin: ferulic and p-coumaric  
523 acids are predominantly linked at the benzyl position of lignin, not the  $\beta$ -position, in grass cell walls,  
524 *Phytochemistry.* 57 (2001) 987–992. doi:10.1016/S0031-9422(01)00052-8.
- 525 [49] V. Becerra, J. Odermatt, M. Nopens, Identification and classification of glucose-based polysaccharides  
526 by applying Py-GC/MS and SIMCA, *J. Anal. Appl. Pyrolysis.* 103 (2013) 42–51.  
527 doi:10.1016/j.jaap.2012.12.018.
- 528 [50] M.J. Prins, K.J. Ptasinski, F.J.J.G. Janssen, Torrefaction of wood: Part 1. Weight loss kinetics, *J. Anal.*  
529 *Appl. Pyrolysis.* 77 (2006) 28–34. doi:10.1016/j.jaap.2006.01.002.
- 530 [51] P.T. Williams, S. Besler, The influence of temperature and heating rate on the slow pyrolysis of biomass,  
531 *Renew. Energy.* 7 (1996) 233–250. doi:10.1016/0960-1481(96)00006-7.
- 532 [52] W.-H. Chen, J. Peng, X.T. Bi, A state-of-the-art review of biomass torrefaction, densification and  
533 applications, *Renew. Sustain. Energy Rev.* 44 (2015) 847–866. doi:10.1016/j.rser.2014.12.039.
- 534 [53] E. Biagini, F. Barontini, L. Tognotti, Devolatilization of Biomass Fuels and Biomass Components  
535 Studied by TG/FTIR Technique, *Ind. Eng. Chem. Res.* 45 (2006) 4486–4493. doi:10.1021/ie0514049.
- 536 [54] D.K. Shen, S. Gu, A.V. Bridgwater, The thermal performance of the polysaccharides extracted from  
537 hardwood: Cellulose and hemicellulose, *Carbohydr. Polym.* 82 (2010) 39–45.  
538 doi:10.1016/j.carbpol.2010.04.018.
- 539 [55] S. Wang, B. Ru, H. Lin, Z. Luo, Degradation mechanism of monosaccharides and xylan under pyrolytic  
540 conditions with theoretic modeling on the energy profiles, *Bioresour. Technol.* 143 (2013) 378–383.  
541 doi:10.1016/j.biortech.2013.06.026.
- 542 [56] S. Wang, B. Ru, H. Lin, W. Sun, Pyrolysis behaviors of four O-acetyl-preserved hemicelluloses isolated  
543 from hardwoods and softwoods, *Fuel.* 150 (2015) 243–251. doi:10.1016/j.fuel.2015.02.045.
- 544 [57] M.S. Mettler, A.D. Paulsen, D.G. Vlachos, P.J. Dauenhauer, Pyrolytic conversion of cellulose to fuels:  
545 levoglucosan deoxygenation via elimination and cyclization within molten biomass, *Energy Environ.*  
546 *Sci.* 5 (2012) 7864–7868. doi:10.1039/C2EE21305B.
- 547 [58] F.-X. Collard, J. Blin, A review on pyrolysis of biomass constituents: Mechanisms and composition of  
548 the products obtained from the conversion of cellulose, hemicelluloses and lignin, *Renew. Sustain.*  
549 *Energy Rev.* 38 (2014) 594–608. doi:10.1016/j.rser.2014.06.013.

- 550 [59] D.K. Shen, S. Gu, A.V. Bridgwater, Study on the pyrolytic behaviour of xylan-based hemicellulose using  
551 TG-FTIR and Py-GC-FTIR, *J. Anal. Appl. Pyrolysis*. 87 (2010) 199–206.  
552 doi:10.1016/j.jaap.2009.12.001.
- 553 [60] C. Branca, C.D. Blasi, C. Mango, I. Hrablay, Products and Kinetics of Glucomannan Pyrolysis, (2013).  
554 doi:10.1021/ie400155x.
- 555 [61] Y. Wu, Z. Zhao, H. Li, F. He, Low temperature pyrolysis characteristics of major components of biomass,  
556 *J. Fuel Chem. Technol.* 37 (2009) 427–432. doi:10.1016/S1872-5813(10)60002-3.
- 557 [62] M. S. Mettler, S. H. Mushrif, A. D. Paulsen, A. D. Javadekar, D. G. Vlachos, P. J. Dauenhauer,  
558 Revealing pyrolysis chemistry for biofuels production: Conversion of cellulose to furans and small  
559 oxygenates, *Energy Environ. Sci.* 5 (2012) 5414–5424. doi:10.1039/C1EE02743C.
- 560 [63] S. Wang, X. Guo, T. Liang, Y. Zhou, Z. Luo, Mechanism research on cellulose pyrolysis by Py-GC/MS  
561 and subsequent density functional theory studies, *Bioresour. Technol.* 104 (2012) 722–728.  
562 doi:10.1016/j.biortech.2011.10.078.
- 563 [64] S. Wang, Z. Xia, Q. Wang, Z. He, H. Li, Mechanism research on the pyrolysis of seaweed  
564 polysaccharides by Py-GC/MS and subsequent density functional theory studies, *J. Anal. Appl.*  
565 *Pyrolysis*. 126 (2017) 118–131. doi:10.1016/j.jaap.2017.06.018.
- 566 [65] M. Kleen, T. Ohra-aho, T. Tamminen, On the interaction of HBT with pulp lignin during mediated  
567 laccase delignification—a study using fractionated pyrolysis-GC/MS, *J. Anal. Appl. Pyrolysis*. 70 (2003)  
568 589–600. doi:10.1016/S0165-2370(03)00028-7.
- 569 [66] J. Rencoret, P. Prinsen, A. Gutiérrez, Á.T. Martínez, J.C. del Río, Isolation and Structural  
570 Characterization of the Milled Wood Lignin, Dioxane Lignin, and Cellulolytic Lignin Preparations from  
571 Brewer's Spent Grain, *J. Agric. Food Chem.* 63 (2015) 603–613. doi:10.1021/jf505808c.  
572